The Comparative Study on Decolorization of Remazol Yellow Dye from Aqueous Solutions by Biosorption, Fenton and Photo-Fenton Processes

N. Ozbay[1], A.S. Yargic[1], M.F. Gozukizil[2], E. Onal[1]

[1] *Department of Chemical and Process Engineering, Bilecik Şeyh Edebali University, Bilecik, 11210, TURKEY.*
[2]*Career School of Pazaryeri, Bilecik Şeyh Edebali University, Bilecik, 11800, TURKEY.*
Corresponding author: seyda.guler@bilecik.edu.tr, Tel: +90 228 214 1244,Fax: +90 228 214 12 22

Abstract

The objective of this study was to investigate *Remazol Yellow* (*RY*) removal under biosorption, Fenton's and photo-Fenton's oxidation processes. *Sunflower pulp* (*SP*) was used as biosorbent; the effects of solution pH, biosorbent dosage, initial dye concentration, contact time, temperature and electrolytes were examined to determine optimum conditions. Under the optimum operating conditions (pH=2, biosorbent dosage=0.1g/50mL solution, initial dye concentration=100ppm), the equilibrium was reached with 69.81% *RY* uptake after 100 min at 20 °C. When 0.2M $CaCl_2 \cdot 2H_2O$ was added to the process, the maximum %dye removal was obtained as 91.18%. The equilibrium data was fitted well to the Langmuir isotherm model. Reaction kinetics was determined to be appropriate to the pseudo-second-order reaction model. According to the thermodynamic parameters, the biosorption process was spontaneous and exothermic under natural conditions. Concentrations of Fe^{+2} and H_2O_2, pH and the use of natural/artificial light were examined to remove color. The maximum decolorization was achieved at pH=3, when concentrations of $FeSO_4$ and H_2O_2 were 80mg/L and100 mg/L, respectively. Experimental results denoted that dye could be effectively decolorized by using Fenton and photo-Fenton processes with high removal efficiencies of 85% and 87%, respectively. According to kinetic modeling of the process performed under optimum conditions, photo-Fenton reaction occurred faster than Fenton reaction. Eventually, Fenton and photo-Fenton reactions are usable techniques for the treatment of textile wastewater with particular interest from the economical point of view. Furthermore, sunflower seed cake can be used as an effective and low-cost biosorbent for dye uptake when attempting to suitable conditions.

Keywords: Biosorption, Fenton, Photo-Fenton, Remazol Yellow.

1. INTRODUCTION

Synthetic organic dyes are used in various industrial processes such as the dyeing of textile fibers, plastic, pharmaceutical, food, cosmetic and printing [1,2]. These dyes are toxic, cause environmental pollution and pose serious hazard to human and aquatic life. Eventually, removing dyes from industrial wastewater sources is an important issue in water purification process for many governments [3,4]. Recently, several techniques have been used to eliminate textile dyes from wastewater, including flocculation combined with flotation, electroflocculation, membrane filtration, electrokinetic coagulation, electrochemical destruction, ion-exchange, irradiation, adsorption, precipitation and ozonation [5]. However, these techniques are generally inefficient in color removal, expensive and less compatible to a wide range of dye wastewater. Biosorption is the reliable technique for the dye removal because of its low capital investment cost, simplicity of design and ease of operation [6]. Many studies have been undertaken to investigate the use of low-cost sorbents such as peat, bentonite, fly ash, silica, bacterial biomass and biopolymers, coir pith, sugar beet pulp, and sugarcane bagasse pith for color removal [7]. Fenton's reagent oxidation is a homogeneous catalytic oxidation process using a mixture of hydrogen peroxide and ferrous ions. The main advantages of the Fenton process are that the chemicals are readily available at moderate cost and there is no need for special equipment [8].

The scope of this study was to investigate *Remazol Yellow* dye uptake by utilizing biosorption, Fenton's and photo-Fenton's oxidation processes. The comparison of effectiveness of these methods on Remazol Yellow dye removal has not yet been studied in the literature. Sunflower *(Helianthus annuus L.)* is cultivated for the production of cooking oil with the total world production of 38 million tons, thus oil industries take out tons of seed cake as biomass material [7]. Sunflower pulp (*SP*) was used as an alternative low-cost sorbent for removal of Remazol Yellow dye from aqueous solutions and it was characterized by proximate analysis, FT-IR and elemental analysis. Optimum biosorption conditions were determined; and also biosorption isotherms, kinetics and thermodynamics were examined. After that, Fenton and photo-Fenton oxidation processes were applied to investigate dye removal. The effects of Fe^{+2} and H_2O_2 concentrations, pH and the use of natural/artificial light were investigated. Finally, kinetic modeling of the advanced oxidation processes was performed and removal efficiencies of three processes were compared.

2. MATERIALS AND METHODS

2.1. Chemicals and Materials

Sunflower pulp (*SP*) attained from Central Anatolia region of Turkey was air-dried, crushed and sieved to obtain a geometrical mean sizes. Bulk density was calculated about 0.47 g/cm^3 for selected size. Carbon, hydrogen, nitrogen and oxygen contents of *SP* were found by using Elemental Analyzer (Leco CNH628 S628). Structure and preliminary analyses were performed to complete the proximate analysis of *SP*. FT-IR spectroscopy was used to identify the chemical groups present in the biosorbent. The infrared spectrum of *SP* was recorded on Perkin Elmer Spectrum 100 in the 4000-400 cm^{-1} wavelength range.
Remazol Yellow (*RY*, color index: Reactive Yellow 15) dye was used without further purification; dye solutions were prepared using distilled water to prevent and minimize possible interferences. Stock solution containing 1000 mg/L of dye was prepared and diluted to arrange different working concentrations. The dye oxidation was achieved by Fenton's reagent which was composed of a mixture of $FeSO_4 \cdot 7H_2O$ (Merck) and H_2O_2 (Merck, 35%). The pH of the reaction mixture was adjusted by adding 1N NaOH and 1N H_2SO_4 solutions. Distilled water from Nüve NS 108 purification system was used throughout this study. Reactions were triggered when hydrogen peroxide was added to reaction mixtures.

2.2. Experimental Procedure

To investigate the effects of pH (2-8), biosorbent dosage (0.05-0.3g/50 mL), initial dye concentration (50-250 mg/L), temperature (293-313 K), contact time (20-120 min) and electrolytes ($NaNO_3$, NH_4NO_3, NaCl and $CaCl_2 \cdot 2H_2O$), batch biosorption experiments were performed in a set of conical flasks containing 50 mL dye solution. After the suspensions were filtered, dye concentrations in the supernatant solutions were measured. A UV-vis spectrum of dye was recorded from 200 to 900 nm using Perkin Elmer Lambda 25 UV-Vis spectrophotometer. The maximum absorbance wavelength (λ_{max}) of *RY* was found to be 422 nm. The dye removal efficiency and the amount of dye sorbed per unit mass can be calculated using following equations [9]:

$$\eta = [(C_0 - C_e)/C_0)100 \quad (1)$$

$$q_e = [(C_0 - C_e)V]/W \quad (2)$$

where C_0 and C_e) (mg/L) are the initial and final concentrations of dye solution, V (L) is the volume of solution and W (g) is the amount of the biosorbent used.

Batch experiments for Fenton and photo-Fenton oxidation were performed in Lovibond Jar Test. UV lamp was used in photo-Fenton process. The initial concentration of dye in the Fenton and photo-Fenton oxidation processes was 100 mg/L and 100 mL of dye solution was used in experiments. The desired quantities of Fe^{2+} and H_2O_2 were added to beakers. The Jar Test apparatus was proceed with rapid mixing of the reaction mixture at 300 rpm for 1 min, slow mixing at 100 rpm for 30 min, and then standstill for 30 min. The effects of solution pH, $FeSO_4 \cdot 7H_2O$ and H_2O_2 dosages on degradation efficiency (%) were investigated. The kinetics of the oxidation was followed by taking samples at regular time intervals. The residual concentration of dyes in the solution was determined by measuring the absorption intensity at maximum absorbance wavelength and degradation efficiency (%) was calculated using Eq. 1.

3. RESULTS AND DISCUSSION

3.1. Biosorbent Characterization

Table 1 represented the ultimate and proximate analysis results of sunflower pulp. According to Table 1, sunflower pulp composed of 10.92% hemicelluloses, 12.53% cellulose, 33.12% lignin, and 23.59% extractive materials. The FT-IR spectrum of the sunflower pulp was given in Fig. 1. Hydroxyl functional groups' O-H stretching vibration including hydrogen bonding was the primary functional group which was detected between 3300 and 3200 cm^{-1}. Symmetric and asymmetric C-H stretching of aliphatic methyl and methylene were detected at 2923 and 2854 cm^{-1}. The carbonyl (-C=O) stretching vibration peaks appeared at 1743.87 and 1640.68 cm^{-1}. Peaks existed at 1535.16 and 1456.27 cm^{-1}

attributed to the aromatic C=C ring stretch. CH=CH stretching was observed at 1235 cm^{-1} and C-O stretching vibrations of lignin were detected at bandwidths of 1100-1000 cm^{-1} [9].

Table 1 Characteristics of *SP*

Ultimate Analysis	
Component	***wt.%***
C	52.15
N	5.19
H	7.42
O[a]	35.26
HHV (MJ/kg)	28.34
Proximate Analysis	
Preliminary analysis	***wt.%***
Moisture	7.72
Ash	6.17
Volatile	75.15
Fixed carbon[a]	10.95
Structural analysis	***w t.%***
Holocellulose	22.90
Hemicellulose	10.92
Extractive material	23.59
Oil	30.30
Lignin	33.12
Cellulose[a]	12.53

[a] Estimated by difference.

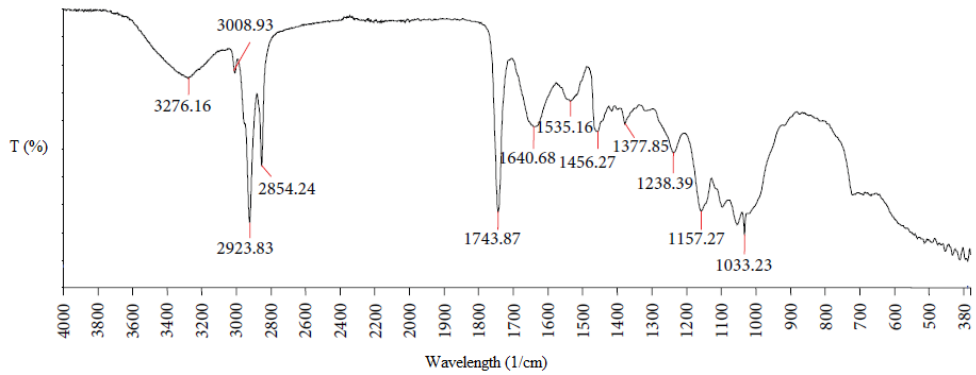

Fig.1 FT-IR spectrum of sunflower pulp

3.2. Biosorption Performance

3.2.1. Effect of solution pH on biosorption

The pH effect on biosorption of dye by *SP* was determined by varying the solution pH from 2 to 8. Fig. 2 showed the removal efficiency for different pHs, when initial dye concentration was 100 mg/L and biosorbent dosage was 0.1 g/50 mL. Maximum biosorption efficiency of 70% was observed at pH 2. This is due to the pH effect on surface charge of the biosorbent; biosorption of anionic species improved as a result of a positive charge on surface developed by acidic conditions [10].

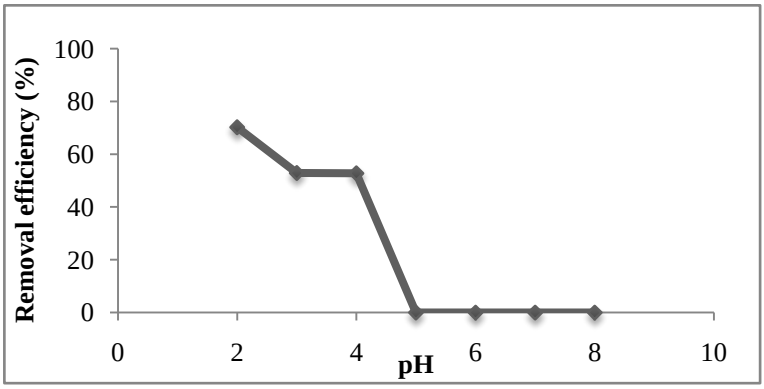

Fig. 2 The pH effect for *RY* biosorption (initial dye concentration: 100 mg/L, contact time: 60 min, temperature: 293 K, biosorbent dosage: 0.1g/50mL dye solution)

3.2.2. Effect of biosorbent dosage on biosorption

Biosorbent dosage determines the capacity of biosorbent for a given initial dye concentration, so it is a considerable parameter for biosorption. Biosorbent dosage effect (0.05-0.3 g/50mL) on *RY* dye biosorption was presented in Fig. 3. The removal efficiency was improved from 46.42% to 88.14% with increasing biosorbent dosage from 0.05 to 0.3g/50mL dye solution. This trend can be predicated to larger surface area and availability of more sorption sites [11].

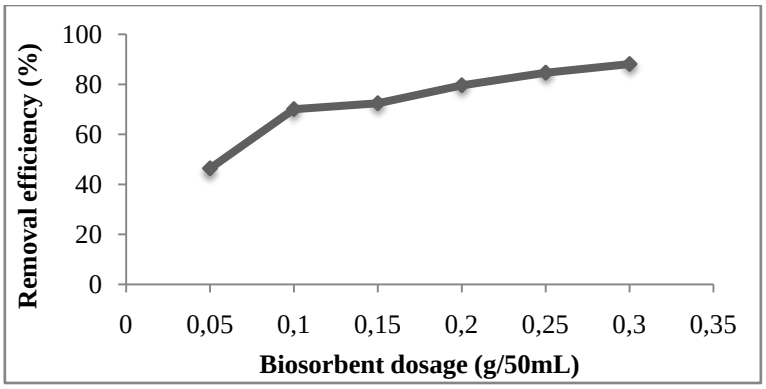

Fig. 3 The biosorbent dosage effect for *RY* biosorption (initial dye concentration: 100mg/L, contact time: 60 min, temperature: 293 K, pH: 2)

3.2.3. Effect of initial dye concentration on biosorption

Fig. 4 showed the effect of initial dye concentration (50-250 mg/L) on the removal efficiency by *SP*. The solution pH was adjusted to the optimum value of 2 and biosorbent dosage was 0.1g/50 mL dye solution. The removal efficiency decreased from 76.33% to 45.53% as the initial dye concentration increased from 50 to 250 mg/L. Biosorption capacity increased as a result of increasing initial dye concentration because the initial dye concentration favors a driving force to accomplish the mass transfer resistance between the solid and aqueous phases [7].

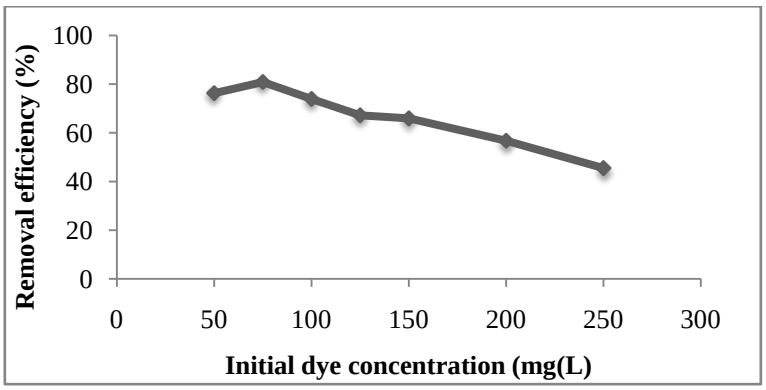

Fig. 4 The initial dye concentration effect for *RY* biosorption (biosorbent dosage: 0.1g/50mL dye solution, contact time: 60 min, temperature: 293 K, pH: 2)

3.2.4. Effect of temperature and contact time on biosorption

Temperature and contact time effects were also studied to decide the equilibrium time of *RY* biosorption onto *SP*. Dye solution with100 mg/L initial concentration was decolorized in an isothermal water bath shaker at 293, 303 and 313 K. At first, biosorbent have a great number of surface sites for biosorption, and then surface sites were occupied by solute molecules [9]. Requisite contact time for *RY* biosorption was found as 80 min (as seen in Fig. 5) and maximum removal efficiency was determined as 69.85% at 293 K. It was decided that the amount of sorbed dye decreased with the increase in temperature indicating that the biosorption reaction of *RY* dye was an exothermic process.

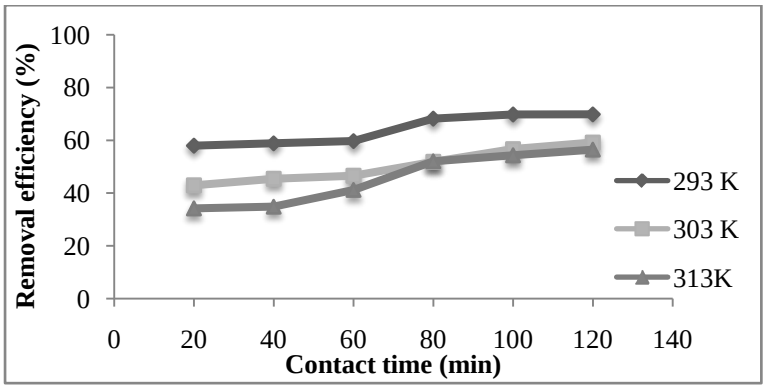

Fig. 5 The temperature and contact time effects for *RY* biosorption (adsorbent dosage:0.1 g/50mL, initial dye concentration: 100mg/L, pH: 2)

3.2.5. Effect of electrolytes on biosorption

Effects of various electrolytes ($NaNO_3$, NH_4NO_3, NaCl, and $CaCl_2 \cdot 2H_2O$) with different concentrations (0.01, 0.05, 0.1, and 0.2 M) on biosorption were investigated. Initial dye concentration was chosen as 100 mg/L and pH was adjusted to 2 to examine electrolyte effects. According to results in Fig. 6, the removal efficiency changed with concentration of electrolytes and electrolyte addition enhanced the dye removal from aqueous solutions. The electrolyte addition affected the removal efficiency positively, which increased to 91.18% when 0.2 M $CaCl_2 \cdot 2H_2O$ was added into the solution. This situation can be explained by the fact that the electrolyte cations neutralize the *SP* surface's negative charge which provides biosorption of more molecules or cations to act directly on the negative adsorbate ions [9].

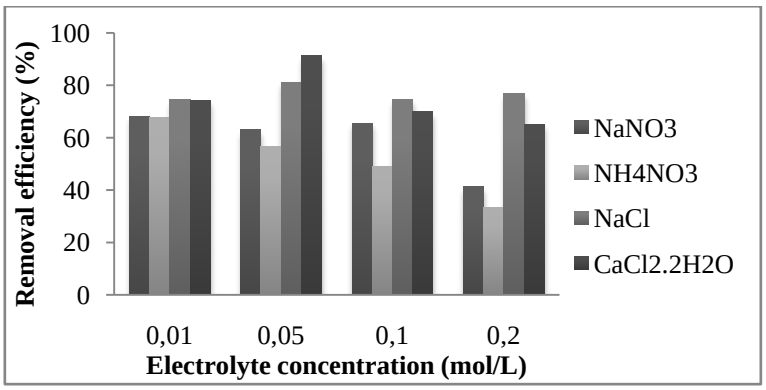

Fig. 6 The electrolyte effect for *RY* biosorption (biosorbent dosage: 0.1 g/50 mL, initial dye concentration: 100 mg/L, pH: 2)

3.2.6. Biosorption isotherms

The relation between the adsorbate concentration in the bulk and the biosorbed amount at the interface was revealed by the adsorption isotherms. The data obtained on the biosorption of *RY* were analyzed by the well-known models given by Langmuir and Freundlich. According to Langmuir model, biosorption is assumed to take place at specific homogeneous sites with the biosorbent; after a dye ion occupies a point, no further biosorption can take place at the point. The Langmuir isotherm is given by the following equation [12]:

$$C_e/q_e = [1/(K_L q_m)] + (C_e/q_m) \quad (3)$$

where q_e (mg/g) is the amount of dye sorbed per unit weight of biosorbent, C_e (mg/L) is the concentration of the dye solution at equilibrium. Also, K_L (L/mg) and q_m (mg/g) are Langmuir constants related to rate of biosorption and maximum biosorption capacity, respectively. K_L and q_m values are obtained from the intercept and the slope of the linear plot of C_e/q_e versus C_e.

The Freundlich isotherm model is used to define the biosorption of an absorbate on a heterogeneous surface of a biosorbent. The mathematical expression of the Freundlich model is given by [13]:

$$\log(q_e) = \log(K_F) + (1/n)\log(C_e) \quad (4)$$

where K_F (mg/g) is a constant related to the biosorption capacity and $1/n$ is an empirical parameter related to the biosorption intensity, which varies with the heterogeneity of material. The intercept K_F and the slope $1/n$ are obtained by plotting $\ln q_e$ versus $\ln C_e$.

Constants and correlation coefficients of the Langmuir model were found as q_m = 2.558 mg/g , K_L = 0.030 L/mg and R^2 = 0.890. Also, the values obtained for Freundlich isotherm model were listed as K_F = 9.023 mg/g, n = 2.469 g/l and R^2 = 0.863. According to correlation coefficients, the Langmuir model displayed better fit to the biosorption data than the Freundlich model. It can be concluded that homogeneous biosorption patches was fulfilled by the interaction between *RY* dye and *SP* surface. Additionally, *SP* could be used to remove the *RY* dye favorably because the heterogeneity factor of n was higher than unity [12].

3.2.7. Biosorption kinetics

Kinetic studies were required to determine the equilibration time for biosorption, thus the Lagergren's pseudo-first and pseudo second order kinetic models were used to investigate the kinetics of *RY* biosorption on *SP*. The pseudo-first order kinetic model is defined as [9].

$$\log(q_e - q_t) = \log(q_e) - [(k_1 t)/2.303] \quad (5)$$

where t is the contact time (min), k_1 is the rate constant of pseudo-first order sorption (min^{-1}), q_e and q_t (mg/g) are the amounts of *RY* biosorbed at equilibrium and at time t (min), respectively. The value of the rate constant (k_1) for *RY* sorption by *SP* was determined from the plot of log ($q_e - q_t$) versus t.

The pseudo-second order model estimates the behavior over the whole range sorption and is also based on the sorption capacity of the solid phase. The pseudo-second order model has a supposition that the sorption process involves chemisorption mechanism and linear form is expresses as [7]:

$$t/q_t = [1/(k_2 q_e^2)] + t/q_e \quad (6)$$

where k_2 is the rate constant of pseudo-second order biosorption (g/mg·min). If pseudo-second order kinetic equation is suitable, q_e and k_2 can be determined experimentally from the slope and intercept of plot t/q_t versus t.

Biosorption rate constants (k_1 *and* k_2), correlation coefficient (R^2) and q_e values for pseudo-first and pseudo-second order kinetic models were given in Table 2. All of the R^2 values for pseudo-second order kinetic model were higher than pseudo-first order kinetic model correlation coefficients. In the case of pseudo-second order kinetics, the calculated $q_{e,cal}$ values was very close to the experimental $q_{e,exp}$ values; that gives agreement that *RY* biosorption on *SP* did not obey the pseudo-first order model. According to kinetic models, biosorption was controlled by a chemisorption mechanism.

Table 2 The pseudo-first and second order kinetic parameters for *RY* biosorption

T (K)	$q_{e,exp}$ (mg/g)	Pseudo-first order kinetic model			Pseudo-second order kinetic model		
		k_1 (min^{-1})	$q_{e,cal}$ (mg/g)	R^2	k_2 (g/(mg·min))	$q_{e,cal}$ (mg/g)	R^2
293	34.926	4.970	35.051	0.615	2.711	37.736	0.992
303	29.587	7.942	28.912	0.710	1.825	32.680	0.982
313	28.237	16.528	29.180	0.723	0.860	35.461	0.954

3.2.8. Biosorption thermodynamics

The changes in thermodynamic parameters such as enthalpy ($\Delta H°$, J/mol), Gibbs free energy ($\Delta G°$, J/mol), and entropy ($\Delta S°$, (J/mol K) for *RY* biosorption process were calculated by using the Van't Hoff equation [12]:

$$\ln K_D = \Delta S°/R - \Delta H°/RT \quad (7)$$

where T is the temperature (K), R is the ideal gas constant (J/mol K), and K_D is the equilibrium constant (L/g). The entropy change ($\Delta S°$) and the enthalpy change ($\Delta H°$) were calculated from a plot of $\ln K_D$ versus $1/T$.

According to slope ($\Delta H°/R$) and intercept ($\Delta S°/R$) the enthalpy change and the entropy change ($\Delta S°$) were found to be -22.25 kJ/mol and -69.39 J/mol.K, respectively. The negative enthalpy change indicated that *RY* biosorption onto *SP* was exothermic, and biosorption rate decreased with increasing temperature. The negative value of $\Delta S°$ showed that the biosorption of *RY* was enthalpy driven and randomness at the biosorbent/adsorbate interface decreased during process. $\Delta G°$ values listed in Table 3 were negative at all three temperatures and increased with increasing temperature. It indicated that thermodynamically biosorption was spontaneous, the spontaneous nature of biosorption become greater with decreasing temperature [12].

Table 3 Thermodynamic parameters for *RY* biosorption onto *SP*

T (K)	$\Delta H°$ (kJ/mol)	$\Delta G°$ (kJ/mol)	$\Delta S°$ (J/mol.K)
293		-1.92	
303	-22.25	-1.23	-69.39
313		-0.53	

3.3. Fenton and Photo-Fenton Performances

3.3.1. Effect of Fe^{2+} dosage

The amount of Fe^{2+} is one of the main parameters affecting the Fenton and photo-Fenton processes. Decolorization efficiencies of *RY* dye were given in Fig. 7 at different ferrous dosages. The experiments were conducted at different concentrations of Fe^{2+} from 10 mg/L to 100 mg/L at a constant H_2O_2 concentration of 60 mg/L. The degradation efficiency increased with a higher initial ferrous concentration, this was because Fe^{2+} ions reacted with H_2O_2 generating more and more •OH radicals which remove the dye by degrading it into smaller molecules [14]. In the presence of 80 mg/L of Fe^{2+} ion, a great improvement of the degradation of *RY* was observed with 68% and 71% degradation efficiencies for both Fenton and photo-Fenton processes. Although, by rising the ferrous dosage from 80 mg/L to 100 mg/L only a small decrease in degradation was established. It may be explained by red-ox reactions that •OH radicals may be scavenged either by the reaction with H_2O_2 present or with another Fe^{2+} molecule to form Fe^{3+} [15].

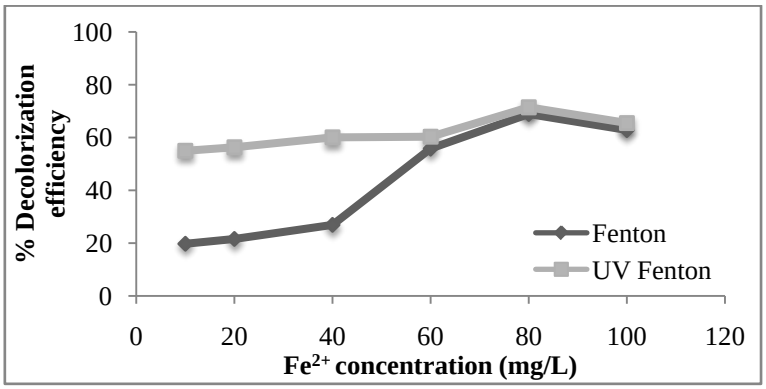

Fig. 7 Effect of ferrous dosage on *RY* degradation by Fenton and photo-Fenton processes

3.3.2. Effect of H_2O_2 dosage

The effect of H_2O_2 dosage on decolorization efficiencies of *RY* dye were given in Fig. 8. pH of reaction mixtures was 2 and the ferrous dosages were used as optimum value of 80 mg/L. The concentration of •OH wass expected to increase with increasing H_2O_2 dosage, leading to increased oxidation rates of organic compounds. When the dosage of H_2O_2 was increased from10 mg/L to 100 mg/L for *RY* removal by Fenton process, the degradation efficiency was not changed considerably and it was also balanced at ~70%. This situation indicated that H_2O_2 alone was not effective in the removal of color [16]. On the contrary, decolorization efficiency increased with H_2O_2 concentration up to maximum value of 92% in photo-Fenton process. Thus, 100 mg/L H_2O_2 was chosen as optimum for both Fenton and photo-Fenton processes.

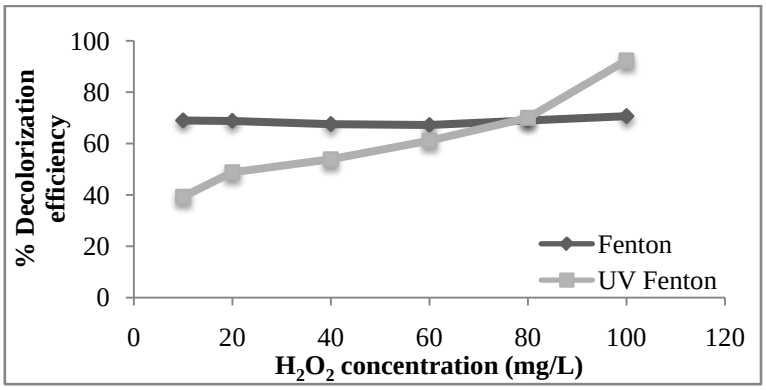

Fig. 8 Effect of hydrogen peroxide dosage on *RY* degradation by Fenton and photo-Fenton processes

3.3.3. Effect of initial pH

The effect of initial pH in the degradation of *RY* dye by Fenton and photo-Fenton oxidation processes was studied in the pH range of 2-8 and the results were shown in Fig. 9. When the initial pH increased from 2 to 3, the removal of *RY* color increased for both Fenton and photo-Fenton processes. The degradation efficiency decreased drastically, when the pH was higher than 3. The reaction rates of Fenton oxidation of dye were rather slow in alkaline medium while they were fast in acidic medium. This result is compatible with the literature where the acidic pH levels (approximately 3.5) are usually optimum for Fenton oxidation [17].

The minimum dye degradation efficiencies at pH=8 were 66.05% and 71.96% for Fenton and photo-Fenton processes, respectively. The formation of ferrous/ferric hydroxide complexes led to the deactivation of ferrous catalyst, so the amount of hydroxyl radical (•OH) generated was very small. At lower pH values, the oxonium ion ($H_3O_2^+$) appeared according to the Eq. 8, this ion elevated the stability of H_2O_2 and limited the •OH formation [18]. The pH value of 3 with 85% and 87% decolorization efficiencies was determined as the optimum for decolorization of *RY* dye by Fenton and photo-Fenton oxidation processes.

$$H_2O_2 + H^+ \rightarrow H_3O_2^+ \quad (8)$$

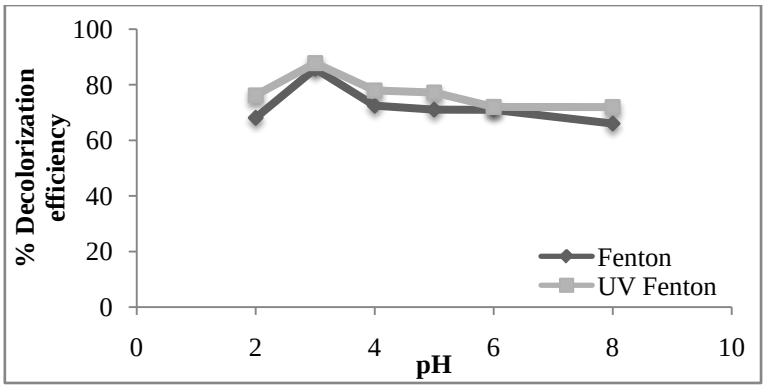

Fig. 9 Effect of pH on *RY* degradation by Fenton and photo-Fenton processes

3.3.4. Fenton and photo-Fenton processes kinetic models

In this study, the decolorization kinetics of *RY* dye by Fenton and photo-Fenton oxidation processes were studied by using Behnajady-Modirshahla-Ghanbery (BMG) reaction kinetics. Behnajady-Modirshahla-Ghanbery (BMG) reaction kinetics is defined as Eq. (9) and (10) [19]:

$$C_t/C_0 = 1 - [t/(m + bt)] \quad (9)$$

$$t/[1 - (C_t/C_0)] = m + bt \quad (10)$$

where b and m are two characteristic constants relating to reaction kinetics and oxidation capacity of process. t is the reaction time, C_0 and C_t are the concentrations of *RY* at initial and any time. A straight line with an intercept of m and a slope of b are obtained by plotting t versus $t/[1 - (C_t/C_0)]$ (see Fig. 10).

Kinetic study was performed at pH=3 with 80 mg/L of Fe^{2+} and 100 mg/L of H_2O_2 concentrations. The BMG kinetic model was found to fit the experimental data well with higher correlation coefficient (R^2) values (Table 4). The physical meaning of 1/*m* was the initial dye discoloration rate in the process. The faster initial discoloration rate of dye could be obtained with the higher 1/*m* value. When *t* was long and approaching infinity, the 1/*b* value indicated the theoretical maximum dye discoloration fraction, which was equal to the maximum oxidation capacity of Fenton process at the end of reaction [20].

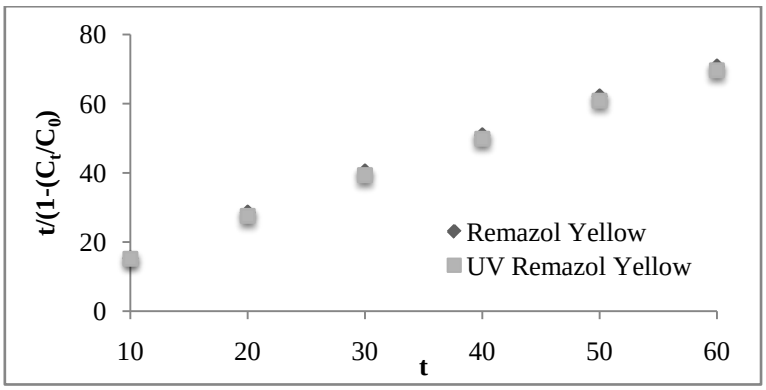

Fig. 10 BMG kinetic model for RY dye by Fenton and photo-Fenton processes

Table 4 The kinetic parameters of Fenton and Photo-Fenton oxidation processes for RY decolorization

	b	***m***	R^2
Fenton	1.109	5.839	0.996
UV-Fenton	1.094	5.438	0.997

4. CONCLUSION

The removal of Remazol Yellow dye from aqueous solutions was performed by using biosorption, Fenton and photo-Fenton processes successfully. Sunflower pulp was a low cost and abundant material that could be used as an alternative biosorbent for reactive dye removal. Solution pH, biosorbent dosage, initial dye concentration, temperature, contact time and electrolytes considerably influenced the biosorption of *RY*. The maximum *RY* removal by biosorption was found as 91.18% under the following conditions: pH=2, biosorbent dosage=0.1g/50mL solution, initial dye concentration=100ppm, contact time=100min, temperature=20°C, electrolyte=0.2M $CaCl_2 \cdot 2H_2O$. The equilibrium data fitted well with Langmuir isotherm model, the kinetic modeling followed the pseudo-second-order kinetic model showing that chemical sorption can control the biosorption. The thermodynamic studies exposed that the biosorption process was spontaneous and exothermic. According to results of dye removal by advanced oxidation processes, optimum Fe^{2+} and H_2O_2 concentrations were found as 80 mg/L and 100 mg/L for both Fenton and photo-Fenton processes at pH value of 3. Under optimum conditions, decolorization efficiencies of Fenton and photo-Fenton processes were 85% and 87%, respectively.

There is no report about comparing conventional biosorption method with advanced oxidation processes to remove reactive Remazol Yellow dye. Experimental results verify that all of the methods including biosorption by sunflower pulp, Fenton and photo-Fenton processes can be used to treat water discharge containing dye such as Remazol Yellow with higher degradation efficiency, when convenient conditions are carried out.

REFERENCES

[1] Bingol, D., Tekin, N., Alkan, M.: Brilliant Yellow dye adsorption onto sepiolite using a full factorial design. Appl. Clay Sci. 50, 315–321 (2010).

[2] He, Y., Gao, J.F., Feng, F.Q., Liu, C., Peng, Y.Z., Wang, S.Y.: The comparative study on the rapid decolorization of azo, anthraquinone and triphenylmethane dyes by zero-valent iron. Chem. Eng. J. 179, 8–18 (2012).

[3] Nawi, M.A., Sabar, S., Jawad, A.H., Sheilatina, Wan Ngah, W.S.: Adsorption of Reactive Red 4 by immobilized chitosan on glass plates: Towards the design of immobilized TiO_2–chitosan synergistic photocatalyst-adsorption bilayer system. Biochem. Eng. J. 49, 317–325 (2010).

[4] Yola, M.L., Eren, T., Atar, N., Wang, S.: Adsorptive and photocatalytic removal of reactive dyes by silver nanoparticle-colemanite ore waste. Chem. Eng. J. 242, 333–340(2014).

[5] Ahmad, M.A., Rahman, N.K.: Equilibrium, kinetics and thermodynamic of Remazol Brilliant Orange 3R dye adsorption on coffee husk-based activated carbon. Chem. Eng. J. 170, 154–161 (2011).

[6] Safa, Y., Bhatti, H.N.: Adsorptive removal of direct textile dyes by low cost agricultural waste: Application of factorial design analysis. Chem. Eng. J. 167, 35–41 (2011).

[7] Yargic, A.S., ,Yarbay Sahin, R.Z., Ozbay, N., Onal, E.: The Effect of Different Operating Conditions on Removal of Reactive Dye by Green Carbon Adsorption. JOSUNAS. 498–510 (2013).

[8] Lucas, M.S., Peres, J.A.: Decolorization of the azo dye Reactive Black 5 by Fenton and photo-Fenton oxidation. Dyes Pigments. 71, 236–244 (2006).
[9] Özbay, N., Yargıç, A.Ş., Yarbay-Şahin, R.Z., Önal, E.: Full factorial experimental design analysis of reactive dye removal by carbon adsorption. J. Chem. 2013, 1–13 (2013).
[10] Santos, S.C., Vilar, V.J., Boaventura, R.A.: Waste metal hydroxide sludge as adsorbent for a reactive dye. J. Hazard. Mater. 153(3), 999–1008 (2008).
[11] Geethakarthi, A., Phanikumar, B.R.: Adsorption of reactive dyes from aqueous solutions by tannery sludge developed activated carbon: Kinetic and equilibrium studies. *Int. J. Environ. Sci. Tech.* 8(3), 561–570 (2011).
[12] Yargıç, A.Ş., Yarbay Şahin, R.Z., Özbay, N., Önal, E.: Assessment of toxic copper (II) biosorption from aqueous solution by chemically-treated tomato waste. J. Clean. Prod. 88, 152–159 (2015).
[13] Javadian, H., Ghaemy, M., Taghavi, M.: Adsorption kinetics, isotherm, and thermodynamics of Hg^{2+} to polyaniline/hexagonal mesoporous silica nanocomposite in water/wastewater. J. Mater. Sci. 49(1), 232–242 (2014).
[14] Fu, F., Wang, Q., Tang, B.: Effective degradation of C.I. Acid Red 73 by advanced Fenton process. J. Hazard. Mater. 174, 17–22 (2010).
[15] Lucas, M.S., Peres, J.A.: Degradation of Reactive Black 5 by Fenton/UV-C and ferrioxalate/H_2O_2/solar light processes. Dyes Pigments. 74, 622–629 (2007).
[16] Kang, S.F., Liao, C.H., Chen, M.C.: Pre-oxidation and coagulation of textile wastewater by the Fenton process. Chemosphere. 46, 923–928 (2002).
[17] Ramirez, J.H., Duarte, F.M., Martins, F.G., Costa, C.A., Madeira, L.M.: Modelling of the synthetic dye Orange II degradation using Fenton's reagent: From batch to continuous reactor operation. Chem. Eng. J. 148, 394–404 (2009).
[18] Sun, S.P., Li, C.J., Sun, J.H., Shi, S.H., Fan, M.H., Zhou, Q.: Decolorization of an azo dye Orange G in aqueous solution by Fenton oxidation process: Effect of system parameters and kinetic study. J. Hazard. Mater. 161, 1052–1057 (2009).
[19] Ertugay, N., Acar, F.N.: Removal of COD and color from Direct Blue 71 azo dye wastewater by Fenton's oxidation: Kinetic study. Arabian J. Chem. Article in press. (2013).
[20] Xu, H.Y., Shi, T.N., Wu, L.C., Qi, S.Y.: Discoloration of Methyl Orange in the Presence of Schorl and H_2O_2: Kinetics and Mechanism. Water, Air, Soil Pollut. 224(10), 1–11 (2013).